

Communication

Review of Asymmetric Seafloor Spreading and Oceanic Ridge Jumps in the South China Sea

Jiangong Wei^{1,2,3,4,†} , Shuangling Dai^{3,†}, Huai Cheng^{1,3,4,*} , Houjin Wang³, Pengcheng Wang⁵, Fuyuan Li³, Zhiyuan Xie^{1,3,4} and Rongwei Zhu³

¹ Sanya Institute of South China Sea Geology, Guangzhou Marine Geological Survey, China Geological Survey, Sanya 572024, China; weijiangong007@163.com (J.W.); xiezhiyuan1990@hotmail.com (Z.X.)

² Zhoushan Field Scientific Observation and Research Station for Marine Geo-Hazards, China Geological Survey, Qingdao 266237, China

³ Key Laboratory of Marine Mineral Resources, Ministry of Natural Resources, Guangzhou Marine Geological Survey, China Geological Survey, Guangzhou 510075, China; daishuangling@mail.cgs.gov.cn (S.D.); whoujin@mail.cgs.gov.cn (H.W.); leefuyuan@sina.com (F.L.); zhurongwei1209@126.com (R.Z.)

⁴ Academy of South China Sea Geological Science, China Geological Survey, Sanya 572024, China

⁵ Key Laboratory of Submarine Geosciences and Prospecting Techniques, Ministry of Education, College of Marine Geosciences, Ocean University of China, Qingdao 266100, China; pengchengwang@ouc.edu.cn

* Correspondence: huai_cheng@126.com

† Jiangong Wei and Shuangling Dai are both regarded as the first author.

Abstract: Seafloor spreading is an important cornerstone of the theory of plate tectonics. Asymmetric seafloor spreading and oceanic ridge jumps are common phenomena in this process and play important roles in controlling oceanic crust accretion, regional tectonics and geological geometric boundaries. As the largest marginal sea in the western Pacific, the South China Sea is an ideal laboratory for dissecting the Wilson cycle of small marginal sea-type ocean basins restricted by surrounding blocks and exploring the deep dynamic processes of confined small ocean basins. In recent years, a lot of research has been conducted on the spreading history of the South China Sea and has achieved fruitful results. However, the detailed dynamic mechanisms of asymmetric seafloor spreading and ridge jumps are still unclear. Therefore, this paper summarizes the basic understanding about the dynamic mechanisms of global asymmetric seafloor spreading and ridge jumps and reviews the related research results of asymmetric seafloor spreading and ridge jumps in the South China Sea. Previous studies have basically confirmed that seafloor spreading in the South China Sea started between ~32 and 34 Ma in the east sub-basin and ended at ~15 Ma in the northwest sub-basin, with at least once oceanic ridge jump in the east sub-basin. The current research mainly focuses on the age of the seafloor spreading in the South China Sea and the location, time and stage of the ridge jumps, but there are relatively few studies on high-resolution lithospheric structure across these ridges and the dynamic mechanism of oceanic ridge jumps. Based on the current research progress, we propose that further studies should focus on the lithosphere–asthenosphere scale in the future, suggesting that marine magnetotelluric and Ocean Bottom Seismometer (OBS) surveys should be conducted across the residual oceanic ridges to perform a detailed analysis of the tectonics magmatism in the east sub-basin to gain insights into the dynamic mechanisms of oceanic ridge jumps and asymmetric seafloor spreading, which can promote understanding of the tectonic evolution of the South China Sea and improve the classical plate tectonics theory that was constructed based on the open ocean basins.

Keywords: South China Sea; east sub-basin; asymmetric seafloor spreading; ridge jumps; dynamic mechanism



Citation: Wei, J.; Dai, S.; Cheng, H.; Wang, H.; Wang, P.; Li, F.; Xie, Z.; Zhu, R. Review of Asymmetric Seafloor Spreading and Oceanic Ridge Jumps in the South China Sea. *J. Mar. Sci. Eng.* **2024**, *12*, 408. <https://doi.org/10.3390/jmse12030408>

Academic Editor: Dmitry A. Ruban

Received: 5 January 2024

Revised: 20 February 2024

Accepted: 21 February 2024

Published: 26 February 2024



Copyright: © 2024 by the authors. Licensee MDPI, Basel, Switzerland. This article is an open access article distributed under the terms and conditions of the Creative Commons Attribution (CC BY) license (<https://creativecommons.org/licenses/by/4.0/>).

1. Introduction

The South China Sea is the largest marginal sea in the western Pacific, strategically located at the junction of the Eurasian Plate, the Pacific Plate and the India–Australian

Plate (Figure 1). It is surrounded by a series of subduction zones and has suffered a complex tectonic evolution from continental margin cracking through seafloor spreading to subduction, including the westward subduction of Pacific Plate, the northeastward subduction of Indo–Australian Plate in the Sumatra Trench and Java Trench, and the southeastward push of the Indochina Block [1–3]. Different from the classic Atlantic type of “intra-plate rifting”, the South China Sea is likely a result of “plate-edge rifting” driven by lithospheric convergence [4–6]. The unique setting makes the South China Sea an ideal laboratory for studying the Wilson cycle in a marginal sea and revealing the deep dynamic process of a confined small ocean basin. Furthermore, improving the awareness of the South China Sea’s “life history” is crucial to comprehend the tectonic evolution and the intricate sea–land interaction process in the western Pacific, which will also help to complement and perfect the plate tectonic theory based on the study of large ocean basins.

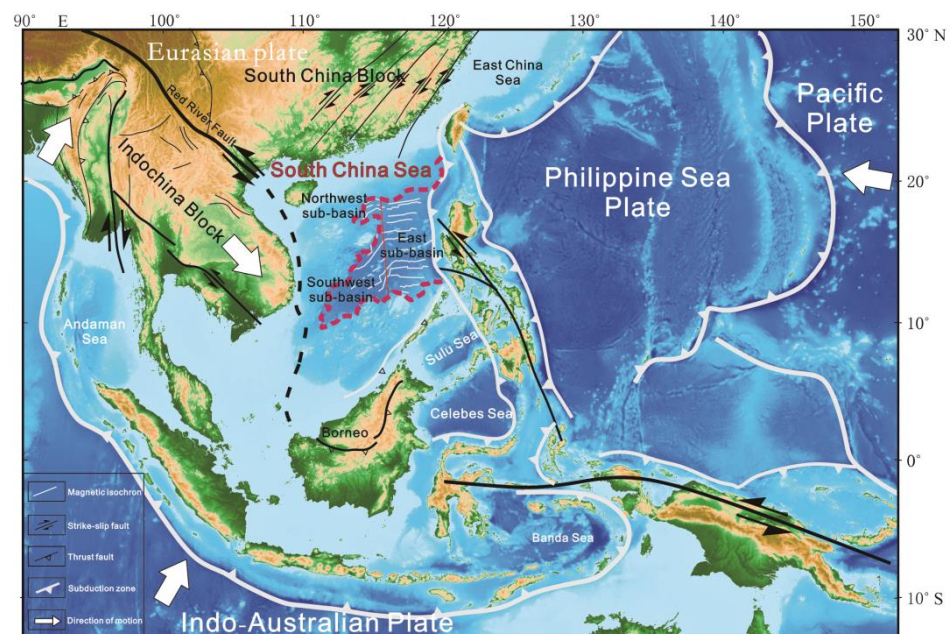


Figure 1. Tectonic setting of the South China Sea (SCS) and adjacent regions, modified from Wang, et al. [2], Villeneuve, et al. [3] and Wang, et al. [7].

Seafloor spreading is a process of continuous accretion of new lithosphere on oceanic ridges, which plays a key role in the evolution of ocean basins and forms an important cornerstone of plate tectonics theory. This process is particularly intriguing in the South China Sea, which is a small ocean basin tightly constrained by the large-scale surrounding plates. In contrast to the spreading observed in large ocean basins like the Atlantic Ocean, the South China Sea’s seafloor spreading exhibits discontinuous and unique characteristics in its spreading type, mode and tectonic properties, potentially highlighting more variable and unsteady features. Therefore, accurately understanding these nuances in seafloor spreading and lithospheric accretion is vital for constructing a comprehensive life history of the South China Sea, shedding light on its unique geological and tectonic evolution.

The study of ridge jumps and asymmetric seafloor spreading, along with their deep dynamic mechanisms, are the key to understanding seafloor spreading progress in the South China Sea. Oceanic ridges, as the primary sites of oceanic lithosphere accretion, showcase the tectono-magmatism that reflects the rheological characteristics and thermal state of the deep mantle. These factors are instrumental in determining the rate and mode of seafloor spreading. During this process, oceanic ridge jump events periodically occur, significantly influencing the geometry, crust–mantle structure and age structure of the ocean basin. Notably, the east sub-basin is the largest sub-basin and the only known place of a ridge jump event in the South China Sea, comprehensively recording the entire progress of asymmetric seafloor spreading. Consequently, the east sub-basin of the South China Sea

presents an excellent opportunity for in-depth studies of ridge jumps, asymmetric seafloor spreading and their deep dynamic mechanisms.

2. Asymmetric Seafloor Spreading and Ridge Jumps

Seafloor spreading is the process of continuous new ocean crust formation at oceanic ridges, which is a crucial aspect of the plate tectonic cycle. Research on spreading rates has led to the classification of oceanic ridges into five categories: ultrafast-spreading (>140 mm/yr), fast-spreading (80–140 mm/yr), intermediate-spreading (55–80 mm/yr), slow-spreading (20–55 mm/yr) and ultraslow-spreading (<20 mm/yr) (Figure 2) [8,9]. Ultrafast- and fast-spreading ridges are typically characterized by dominant magmatism. Here, high crustal temperature stabilizes the lower part of the magma chamber, forming a central uplift with relatively low topography, as exemplified by the East Pacific Rise [10,11]. In contrast, slow- and ultraslow-spreading ridges are usually dominated by tectonic processes with limited magma supply. These ridges often feature a significant central rift marked by distinct segmentation, commonly seen in the Atlantic Ocean, the southwest Indian Ocean, the Arctic Ocean, etc. [12–16]. Intermediate-spreading ridges represent a balance between these extremes, where the development of magma chambers at the lower part of oceanic ridges coexists with extensive fault structures.

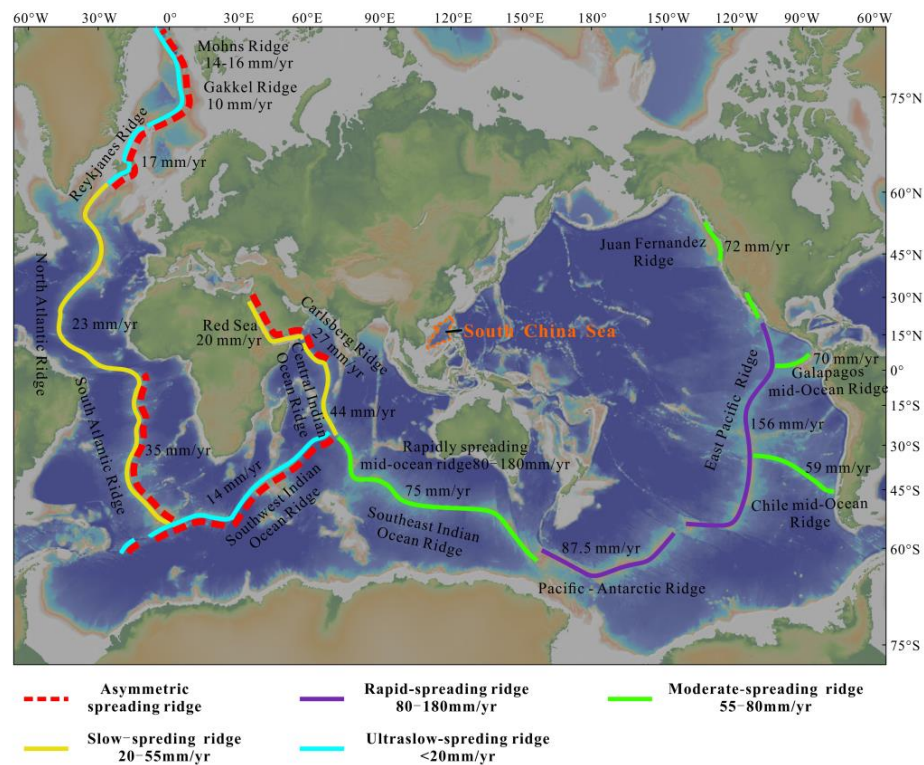


Figure 2. Map showing the distribution and classification of global mid-oceanic ridges (data on the total spreading rate of mid-oceanic ridges are from DeMets, et al. [17]).

Seafloor spreading is primarily categorized into two types: symmetric and asymmetric spreading (Figure 2). Asymmetric spreading is characterized by different spreading rates and crustal structures on both sides of the oceanic ridge [18–23], which is a common spreading mode in slow- and ultraslow-spreading oceanic ridges and can be extensively observed in regions such as the Arctic Ocean, southwest Indian Ocean, northwest Indian Ocean and south Atlantic Ocean [18,24–26]. Compared with symmetric spreading, asymmetric spreading has a more complex and dynamic mechanism. Regionally, asymmetric spreading often correlates with hotspots [14], predominantly driven by variations in deep magma supply [27]. Locally, factors such as magmatic activity, spreading rates and the specific tectonic setting influence the asymmetry of seafloor spreading [16,19,28–31].

Ridge jumps are frequent events during seafloor spreading, representing the death of old oceanic ridges and the birth of new oceanic ridges. This phenomenon significantly influences ocean crust accretion, regional structures and the geological geometric boundaries [32]. Therefore, determining the time and stages of ridge jump events is crucial for reconstructing the tectonic evolution of ocean basins, and it plays a key role in comprehending the development and sedimentary infill of continental margin basins. At present, accurate division of seafloor magnetic anomaly bands is the main means to identify oceanic ridge jumps. For instance, the magnetic anomaly bands on the Atlantic seabed indicate that the A2 ridge has shifted eastward 20–25 km since 1 Ma [33,34]. Generally, a ridge jump requires the concurrent presence of two factors: a reduction in the lithospheric strength and a stress field conducive to lithospheric rupture beyond the ridge.

The interaction between mantle plumes and oceanic ridges is one of the main dynamic mechanisms of oceanic ridge jumps, primarily manifested through the thermo-mechanical erosion and shearing effects of magma upwelling on the lithosphere, which can cause the oceanic ridges to jump towards the hotspots [35–37]. Typically, ridge jump events tend to occur in the younger lithospheres with slower spreading rates. For instance, the Indian Ocean experienced two significant ridge jumps around 120–87 Ma and 70–65 Ma. And the direction of these jumps was consistent with the relative movement direction of the hotspot and the plate, indicating the substantial impact of plume–oceanic ridge interaction on ridge jumps [38]. Another dynamic mechanism driving oceanic ridge jumps is plate subduction, where the lithosphere is stretched by far-field tectonic stress and melt generated from the lithospheric mantle to induce the oceanic ridge jump [39].

Previous research on oceanic ridge jumps has predominantly centered on large ocean basins, with limited focus on the specific processes and mechanisms of these jumps in smaller marginal ocean basins influenced by “plate edge rifting”. Therefore, it is urgent to conduct detailed studies in representative marginal seas to gain a more comprehensive understanding of oceanic ridge jumps in these unique settings.

3. Asymmetric Seafloor Spreading and Ridge Jumps in the South China Sea

The South China Sea is the largest marginal sea in the western Pacific, surrounded by the Eurasian Plate, the Indo–Australian Plate and the Philippine Sea Plate, with several subduction zones developing around it (Figure 1). Since the late Jurassic to early Cretaceous, a great Mesozoic ocean had subducted obliquely beneath the Eurasian continent and generated a Mesozoic massive magmatic arc around the Cathaysia Block (Figure 3a) [40]. At ~40 Ma, the southward subduction of the Proto-South China Sea generated the NE–SE extensional faults and arc magma in the Philippine islands (Figure 3b), then led to lithospheric stretching along the Eurasian/Huatung Plate boundary to develop the South China Sea at ~33 Ma (Figure 3c) [40,41]. Generally, the geological history of the South China Sea includes continental margin rifting since the late Cretaceous (Figure 3a,b), followed by seafloor spreading from the early Oligocene to early Miocene (Figure 3c–e), and transitioning into subduction under the Philippine Sea Plate in the middle Miocene (Figure 3f–h) [1]. A total of three secondary ocean basins have developed in the South China Sea, namely the northwest sub-basin, the east sub-basin and the southwest sub-basin (Figure 4). Initially, seafloor spreading in the South China Sea began in the northwest and east sub-basins, predominantly in an N–S direction. Later, a shift in the oceanic crust spreading axis led to the gradual opening of the southwest sub-basin, with the spreading center extending in an N–S direction and spreading progressively from east to west [42–48]. These basins have undergone an evolution process of early uniform fault subsidence to middle and late detachment fault subsidence in the synrift stage, indicating that the differentiated detachment along large faults is pivotal in the lithosphere’s critical rupture process [48–53]. Generally, in contrast to the Atlantic Ocean, which is characterized by a stable spreading center and a symmetrical continental margin, the spreading of the South China Sea Basin is controlled by the surrounding large-scale plates (such as the Eurasia Plate, the Indo–Australia Plate, etc.), and belongs to a restricted small ocean basin with characteristics of a small-scale, new age, and complex spreading process [54,55].

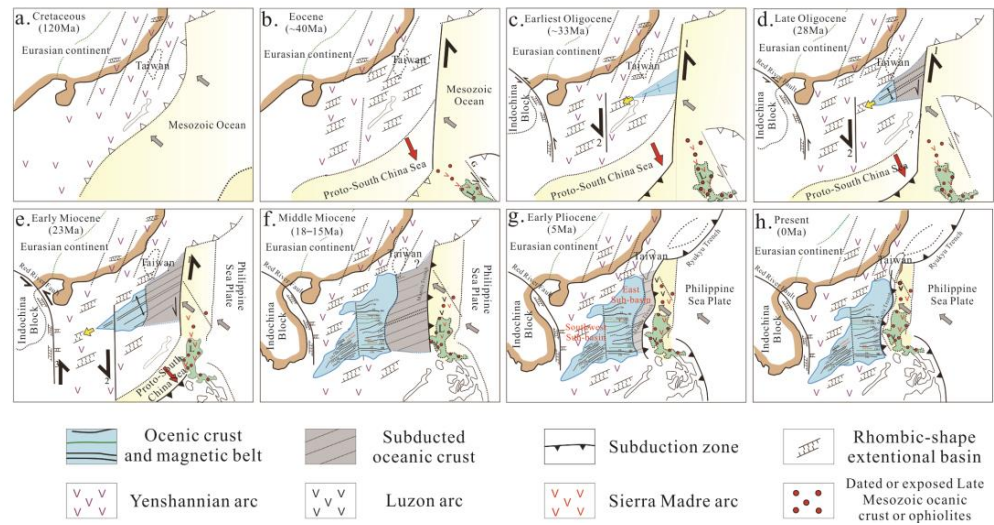


Figure 3. A proposed strike–slip mechanism to open up the SCS and tectonic processes, modified from Huang, et al. [40]. A great Mesozoic ocean (yellow color) was progressively consumed when the SCS (blue and gray colors) and the WPB (white region) were developing on both sides of the Huatung Basin. For details of the evolution processes, see the text part. The red arrows indicate the direction of plate movement. The black half arrows indicate the direction of the fault strike–slip. L, Luzon.

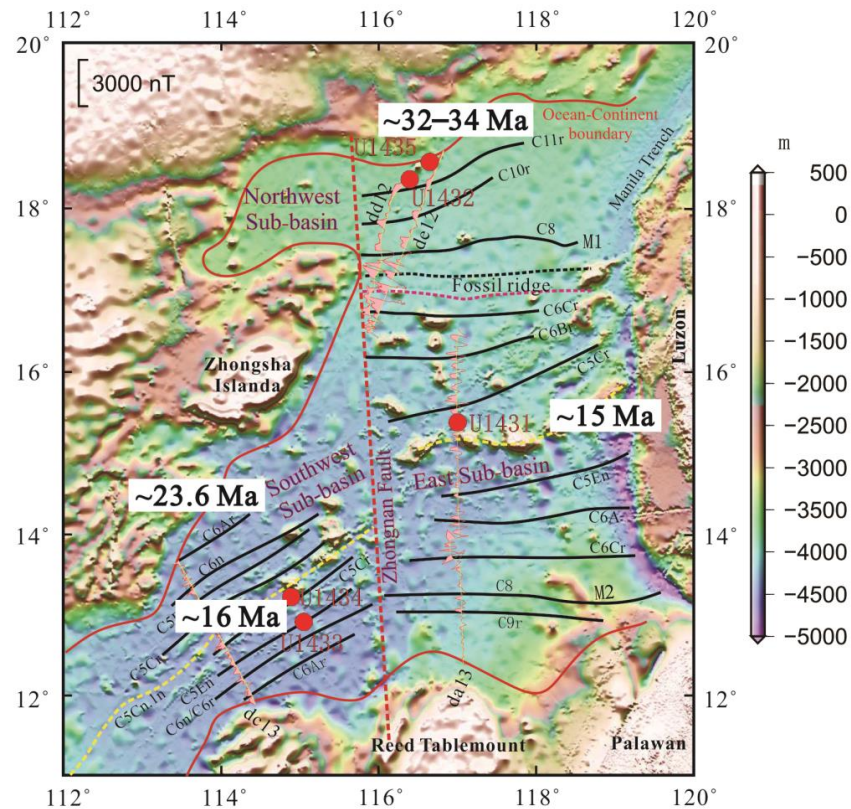


Figure 4. Bathymetry map of the South China Sea showing the first deep-tow magnetic survey tracks (dd12, de12, da13 and dc13), magnetic isochrons (shown with black lines and black chron labels) and 5 drilling cores in IODP349 (shown with red dots). Combined analyses of deep-tow magnetic anomalies and IODP349 cores show that initial seafloor spreading started ~32–34 Ma in the east sub-basin and ~23.6 Ma in the southwest sub-basin, and ended ~16 Ma in the southwest sub-basin and ~15 Ma in the east sub-basin, modified from Li, et al. [56]. The solid red line is the boundary of the South China Sea Basin. The yellow dashed lines indicate the relict spreading center in the southwest sub-basin and east sub-basin, respectively.

The seafloor spreading age in the South China Sea has long been the focus of geological research [43–45,55–61]. Magnetic anomaly bands are key to recording the timeline of this seafloor spreading. However, the accuracy of the spreading age derived exclusively from these bands is compromised due to factors such as data quality and subsequent magmatic activity. Previous studies have proposed different age models of 32–17 Ma, 32–15.5 Ma, 31–20.5 Ma, etc. [43–45,60,61]. Based on the deep-towed geomagnetic data of the “South China Sea Deep” project and basement basalt sample dating from the International Ocean Discovery Program (IODP) drilling, the initiation and cessation of seafloor spreading in the South China Sea were determined to be 32–34 Ma and 15 Ma, respectively. The cessation of seafloor spreading in the east and southwest sub-basins are ~15 Ma and ~16 Ma, respectively (Figure 4) [42,56,59,62]. Furthermore, the identification of seismic unconformity surfaces in South China Sea has helped to reconstruct the spatio-temporal pattern of ocean basin spreading [48]. For instance, the rupture unconformity surface in the eastern part of the South China Sea was first formed at ~34 Ma [48,63]. The most prominent unconformity surface in the central part occurred at 23.6 Ma, indicating the beginning of spreading near the southwest sub-basin [48]. The latest rupture unconformity surface in the western part was formed at ~16 Ma, which coincides with the cessation of spreading in the southwest sub-basin, showing a migration from east to southwest [48,63–67]. On the whole, the results of magnetic isochrons, IODP drilling and unconformity surfaces show that the onset of seafloor spreading in the South China Sea began between 32 and 34 Ma and ended around 15 Ma, and the final crustal rupture and the start of seafloor spreading did not occur simultaneously from east to west, but expanded progressively in a “V” shape from east to west (Figure 3c–f).

The eastern sub-basin is the largest sub-basin in the South China Sea (Figure 1), and its developmental history runs through the entire spreading process of the South China Sea Basin. Asymmetric spreading and ridge jumps are the most important characteristics in the east sub-basin. Magnetic anomaly bands, bathymetric data and gravity anomalies indicate that seafloor spreading in the east sub-basin shows asymmetric characteristics (Figure 5). With the residual ridge where the Zhenbei-Huangyan seamount chain is located as the boundary, some magnetic anomaly strips are missing on the southern wing of the east sub-basin, and the magnetic anomaly bands on the northern wing are discontinuous [43,68]. The uneven distribution of such magnetic anomaly bands indicates the existence of asymmetry in seafloor spreading (Figure 5a). The water depth data and the ocean-continent boundary identified by seismic measurement also show that the east sub-basin is geometrically asymmetrical with “width in the north and narrow in the south” [69]. Besides, the residual mantle bouguer gravity anomaly (RMBA) of the eastern subbasin (Figure 5b) and retrieved the oceanic crust thickness (Figure 5c) calculated by gravity and sediment data also point out that there is an obvious north-south asymmetry in the RMBA and oceanic crust thickness on both sides of the residual ocean ridge, indicating that the northern side has higher mantle temperature and more magma activity than the south side, reflecting the asymmetry of the deep structure (Figure 5d) [70,71]. It can be seen that the structure of South China Sea lithosphere from lateral to the vertical directions shows the asymmetric characteristics of seafloor spreading.

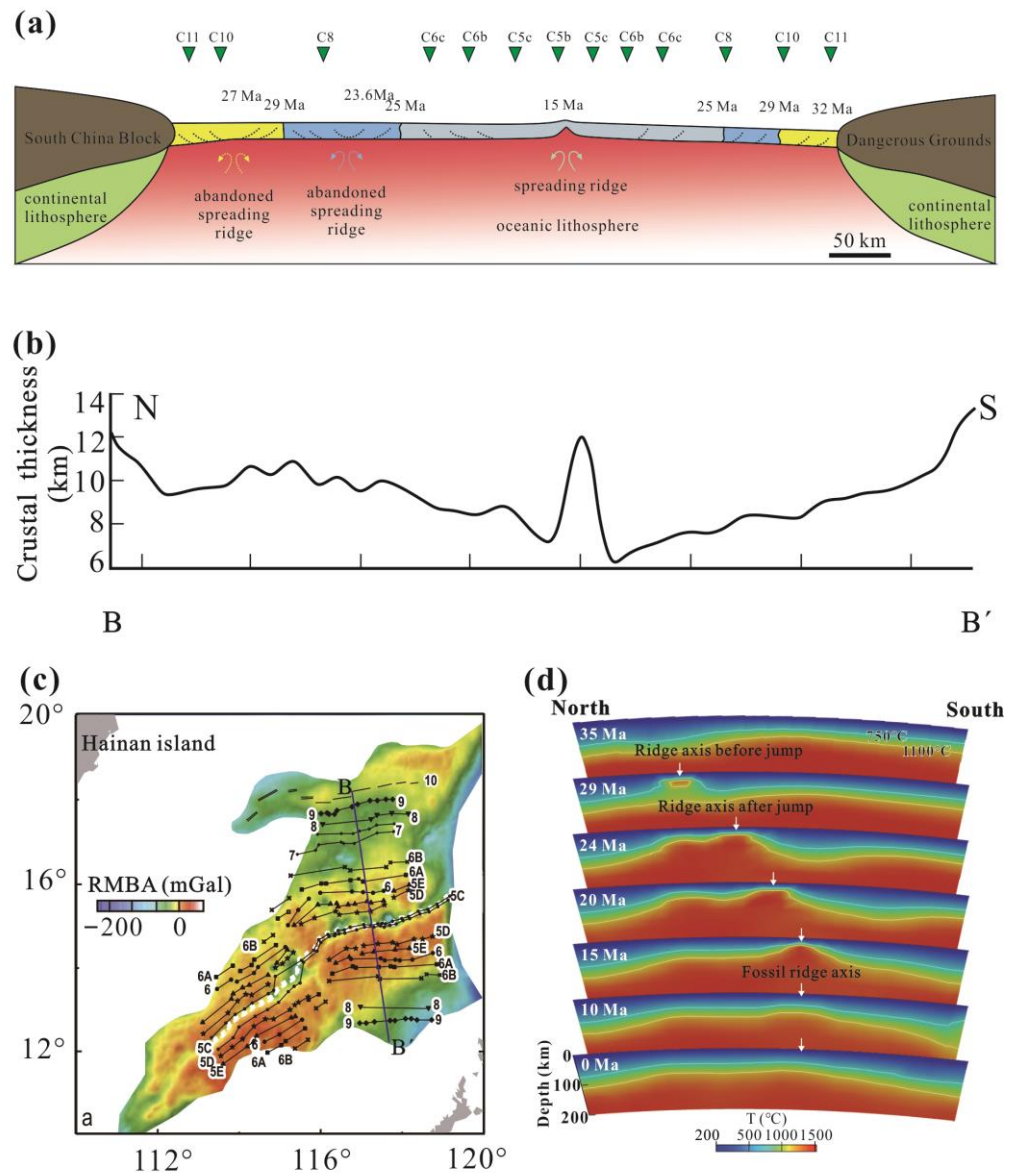


Figure 5. Characteristics of asymmetric structure in the eastern sub-basin of the South China Sea. (a) Magnetic anomalies, modified from Ding, et al. [69]; (b) Changes in crustal thickness, profile B-B' location is shown in (c), modified from Ding, et al. [70]; (c) Calculated residual mantle Bouguer anomaly (RMBA), modified from Zhang, et al. [71]; (d) Calculated changes in mantle temperature, profile direction is similar to B-B', modified from Lin, et al. [72].

Ridge jumps are significant events in the spreading history of the east sub-basin. However, the location, time and stage of these ridge jumps remain a topic of debate. At present, most researchers agree that ridge jumps have occurred in the east sub-basin of the South China Sea, but they diverge in their interpretations of the timing (Figure 6a). Taylor and Hayes [44] posited a southward ridge jump at 27 Ma (magnetic anomaly band C7a). In contrast, Briais, et al. [43] and Barckhausen, et al. [61] concurred with the occurrence of a ridge jump but date it around 25 Ma. Based on high-precision deep-drag geomagnetic detection and seismic profile analysis, Li, et al. [56] suggested that the oceanic ridge shifted southward by approximately 20 km at 23.6 Ma. In addition, some scholars have proposed the idea that there were two or more oceanic ridge jumps that occurred in the east sub-basin. Ding, et al. [69] deduced that two southward ridge jumps occurred at 27 Ma and 23.6 Ma based on deep reflection seismic analysis revealing two sets of opposite-dipping lower crustal reflectors (LCR) on the northern side of the ridge (Figure 6b).

However, Wen, et al. [73] proposed a different interpretation of these reflectors, suggesting they might represent magmatic intrusions accumulated in partially serpentinized mantle during the latest rifting before lithosphere breakup, or magmatic relicts in the paleo-melt transfer channels and/or frozen molten materials in the shear zone of lithospheric and asthenospheric mantle, formed before the onset of mature seafloor spreading. In addition, based on the high-resolution magnetic anomaly bands, Guan, et al. [74] suggested that the east sub-basin underwent five successive ridge jumps at ~28 Ma (C9r), ~25.9 Ma (C8n), ~25 Ma (C7n), ~19.9 Ma (C6n) and ~18.5 Ma (C5En), and the direction of spreading changed during the ridge jumps (Figure 6c).

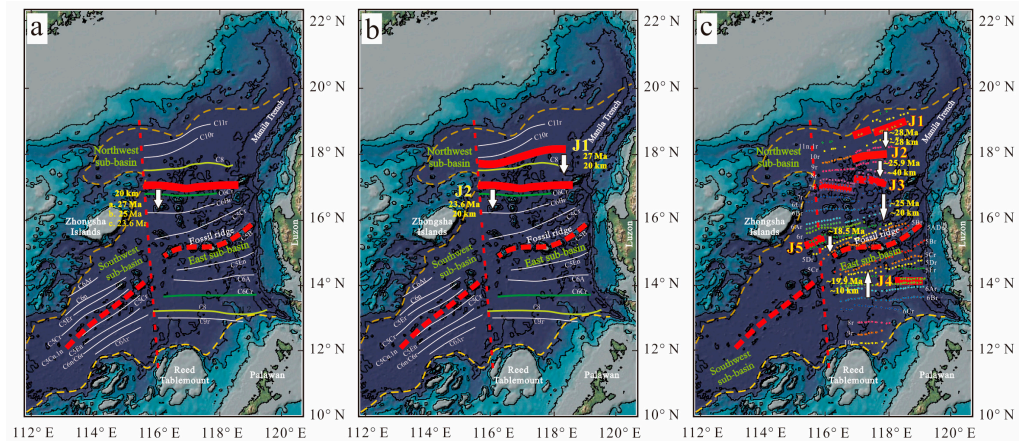


Figure 6. Map showing the time, position and period of mid-oceanic ridge jumps in the South China Sea. (a) One ridge jump displaced the ridge ~20 km southward, which may have occurred at 27 Ma [44], 25 Ma [43,61] and 23.6 Ma [56]; (b) Two ridge jumps: the first ridge jump occurred at ~27 Ma displacing the ridge ~20 km southward; the second southward ridge jump event occurred at ~23.6 Ma, also with a 20 km offset [69]; (c) Five ridge jumps: the positions of the ridge jumps are shown with thick red lines and are labelled with J1–J5. The ridge jumps occurred at ~28 Ma (C9r), ~25.9 Ma (C8n), ~25 Ma (C7n), ~19.9 Ma (C6n) and ~18.5 Ma (C5En), respectively [74]. The white arrows indicate the direction of range jump. The red solid lines indicate the fossil ocean ridge. The red dashed lines indicate the last residual ocean ridge now. The colored dotted lines indicate the magnetic anomaly bands.

There is a close relationship between the ridge jumps and asymmetric spreading in the east sub-basin of the South China Sea. During the discontinuous asymmetric spreading process of the east sub-basin, not only did the ridge jumps occur, but also the direction of spreading changed. These ridge jumps resulted in geometrically asymmetric structures with a wide northern limb and a narrow southern limb of the east sub-basin [75]. Geodynamic numerical simulations have led to the hypothesis that partial melting occurred in the lower region between the old and new oceanic ridges, causing higher mantle temperatures and more intense magmatic activity on the northern side of the spreading center, thereby creating a deep structural asymmetry [76]. However, the dynamic mechanisms of ridge jumps and asymmetric seafloor spreading are still not fully understood. Ding [75] postulated that the periodic deep magma activity in the mantle, coupled with shifts in the location of magma upwelling could trigger these ridge jumps. Therefore, comprehension of the processes and distribution of deep magma, as well as the relationship between structure and magmatism, might be the key to unraveling the complexities of the dynamic mechanisms driving oceanic ridge jumps and asymmetric spreading.

4. Conclusions and Future Prospects

After long-term investigation and research, especially the implementation of the “South China Sea Deep” project and multiple South China Sea drilling cruises by IODP, significant insights have been gained about the spreading history of the South China Sea.

Comprehensive analysis of ocean drilling cores and deep-tow magnetic anomalies have established that the South China Sea spreading started between 32 and 34 Ma and ended around 15 Ma. And at least one southward spreading ridge jump has occurred in the South China Sea. However, limitations in the fusion of geophysical data and the detection depth of geophysical exploration equipment have constrained our understanding of ridge jumps, asymmetric seafloor spreading processes and their underlying dynamic mechanisms. There are two primary challenges in this area of research. Firstly, there is a noticeable absence of cross-validation among the data and research methodologies used by different researchers. Second, most existing studies rely predominantly on crustal-scale geophysical data, which lacks the depth and precision required for more comprehensive insights. Given these challenges, it is urgent to introduce new methods and data to conduct in-depth research from the lithosphere to asthenosphere scale so as to answer important scientific questions such as the location of residual oceanic ridges at different times, the duration and mode of oceanic ridge jumps and the dynamic mechanisms of oceanic ridge jumps and asymmetric seafloor spreading.

In recent years, the marine magnetotelluric method has achieved great success in revealing the structures of oceanic ridges. Key, et al. [77] and Johansen, et al. [27] conducted comprehensive magnetotelluric surveys at the north side of the East Pacific Rise and the Mohs Ridge of the Arctic Ocean, respectively. Their work successfully delineated key features such as Moho, the lithosphere–asthenosphere interface (LAB) and magma migration channels beneath the active oceanic ridges. This research sets a valuable precedent for in-depth studies of the crust and asthenosphere, particularly in regions like the South China Sea. In 2020, the Guangzhou Marine Geological Survey successfully undertook a 260 km deep marine magnetotellurism survey across the southwest sub-basin. This survey gathered detailed electrical and thermal structure profiles reaching down to the asthenosphere. This effort not only marks a significant advancement in ocean magnetotelluric data acquisition but also in the processing and interpretation methodologies [78]. Complementing these efforts, active source OBS refraction travel time tomography has emerged as a crucial method for inverting the velocity structure of the crust [79–81], which can effectively make up for the lack of marine magnetotelluric ability in resolving shallow structures.

For future research on asymmetric seafloor spreading and ridge jumps in the east sub-basin of the South China Sea, a strategic approach is recommended. This involves focusing on the detailed characterization of the crust–mantle structure extending to the asthenosphere. To achieve this, it is crucial to collect both magnetotelluric data and active source OBS data from residual oceanic ridges across different periods in the east sub-basin. This data collection should be integrated with existing comprehensive geophysical data, including gravity, magnetic and seismic records. In addition, incorporating thermo-mechanical numerical simulations will enhance the analysis. Through a multidisciplinary approach combining multiple methods and datasets, this integrated strategy aims to unravel the processes of oceanic ridge jumps and asymmetric seafloor spreading in the South China Sea, along with their deep dynamic mechanisms.

Author Contributions: Conceptualization, J.W. and H.C.; formal analysis, H.W., F.L. and P.W.; data curation, Z.X. and R.Z.; writing—original draft preparation, J.W., H.C., S.D. and H.W.; writing—review and editing, J.W., H.C. and F.L.; visualization, P.W., Z.X., S.D. and R.Z. All authors have read and agreed to the published version of the manuscript.

Funding: This study was supported by the National Key R&D Program of China (2021YFC2800300), the open research fund program of Zhoushan Field Scientific Observation and Research Station for Marine Geo-hazards, the China Geological Survey (No. ZSORS-22-03), the China Geological Survey Project (grant number DD20230404), and the Guangzhou Science and Technology Project (No. 2023A04J0235).

Institutional Review Board Statement: Not applicable.

Informed Consent Statement: Not applicable.

Data Availability Statement: The data presented in this study are available in the cited references.

Acknowledgments: We would like to thank the Guangzhou Marine Geological Survey (GMGS) for allowing the data of this research to be shared. We are grateful to Michel Villeneuve and one anonymous reviewer for constructive and insightful comments that have improved the manuscript significantly.

Conflicts of Interest: The authors declare no conflicts of interest.

References

1. Savva, D.; Pubellier, M.; Franke, D.; Chamot-Rooke, N.; Meresse, F.; Steuer, S.; Auxietre, J.-L. Different expressions of rifting on the South China Sea margins. *Mar. Pet. Geol.* **2014**, *58*, 579–598. [[CrossRef](#)]
2. Wang, P.; Li, S.; Suo, Y.; Guo, L.; Santosh, M.; Li, X.; Wang, G.; Jiang, Z.; Liu, B.; Zhou, J. Structural and kinematic analysis of Cenozoic rift basins in South China Sea: A synthesis. *Earth-Sci. Rev.* **2021**, *216*, 103522. [[CrossRef](#)]
3. Villeneuve, M.; Martini, R.; Bellon, H.; Réhault, J.-P.; Cornée, J.-J.; Bellier, O.; Burhannuddin, S.; Hirschberger, F.; Honthaas, C.; Monnier, C. Deciphering of six blocks of Gondwanan origin within Eastern Indonesia (South East Asia). *Gondwana Res.* **2010**, *18*, 420–437. [[CrossRef](#)]
4. Wang, P.; Huang, C.-Y.; Lin, J.; Jian, Z.; Sun, Z.; Zhao, M. The South China Sea is not a mini-Atlantic: Plate-edge rifting vs intra-plate rifting. *Natl. Sci. Rev.* **2019**, *6*, 902–913. [[CrossRef](#)] [[PubMed](#)]
5. Wang, P. Exploring the deep sea processes in the South China Sea. *Sci. Technol. Rev.* **2020**, *38*, 6–20. [[CrossRef](#)]
6. Lin, J.; Sun, Z.; Li, J.; Zhou, Z.; Zhang, F.; Luo, Y. South China Seabasin opening: Lithospheric rifting and interaction with surrounding subduction zones. *Sci. Technol. Rev.* **2020**, *38*, 35–39. [[CrossRef](#)]
7. Wang, P.; Li, S.; Suo, Y.; Guo, L.; Wang, G.; Hui, G.; Santosh, M.; Somerville, I.D.; Cao, X.; Li, Y. Plate tectonic control on the formation and tectonic migration of Cenozoic basins in northern margin of the South China Sea. *Geosci. Front.* **2020**, *11*, 1231–1251. [[CrossRef](#)]
8. Dick, H.J.B.; Lin, J.; Schouten, H. An ultraslow-spreading class of ocean ridge. *Nature* **2003**, *426*, 405–412. [[CrossRef](#)] [[PubMed](#)]
9. Macdonald, K.C. Mid-ocean ridges: Fine scale tectonic, volcanic and hydrothermal processes within the plate boundary zone. *Annu. Rev. Earth Planet. Sci.* **1982**, *10*, 155. [[CrossRef](#)]
10. White, R.S.; Detrick, R.S.; Mutter, J.C.; Buhl, P.; Minshull, T.A.; Morris, E. New seismic images of oceanic crustal structure. *Geology* **1990**, *18*, 462–465. [[CrossRef](#)]
11. Li, Y.; Niu, X.; Ruan, A.; Liu, S.; Haider, S.W.; Wei, X. On spreading rates and crustal structure at mid-ocean ridges. *Chin. J. Geophys.* **2020**, *63*, 1913–1926. [[CrossRef](#)]
12. Cannat, M.; Sauter, D.; Mendel, V.; Ruellan, E.; Okino, K.; Escartin, J.; Combier, V.; Baala, M. Modes of seafloor generation at a melt-poor ultraslow-spreading ridge. *Geology* **2006**, *34*, 605–608. [[CrossRef](#)]
13. Edmonds, H.; Michael, P.; Baker, E.; Connelly, D.; Snow, J.; Langmuir, C.; Dick, H.; Mühe, R.; German, C.; Graham, D. Discovery of abundant hydrothermal venting on the ultraslow-spreading Gakkel ridge in the Arctic Ocean. *Nature* **2003**, *421*, 252–256. [[CrossRef](#)] [[PubMed](#)]
14. Sauter, D.; Cannat, M.; Meyzen, C.; Bezos, A.; Patriat, P.; Humler, E.; Debayle, E. Propagation of a melting anomaly along the ultraslow Southwest Indian Ridge between 46° E and 52°20' E: Interaction with the Crozet hotspot? *Geophys. J. Int.* **2009**, *179*, 687–699. [[CrossRef](#)]
15. Schroeder, T.; Cheadle, M.J.; Dick, H.J.; Faul, U.; Casey, J.F.; Kelemen, P.B. Nonvolcanic seafloor spreading and corner-flow rotation accommodated by extensional faulting at 15 N on the Mid-Atlantic Ridge: A structural synthesis of ODP Leg 209. *Geochem. Geophys. Geosyst.* **2007**, *8*, Q06015. [[CrossRef](#)]
16. Ling, Z.; Gao, J.; Zhao, L.; Yang, C.; Guan, Q.; Zhang, T. The asymmetric crustal structures of basement ridges of the Gakkel Ridge. *Chin. J. Geophys.* **2019**, *62*, 1755–1771. [[CrossRef](#)]
17. DeMets, C.; Gordon, R.G.; Argus, D.F. Geologically current plate motions. *Geophys. J. Int.* **2010**, *181*, 1–80. [[CrossRef](#)]
18. Escartin, J.; Smith, D.K.; Cann, J.; Schouten, H.; Langmuir, C.H.; Escrig, S. Central role of detachment faults in accretion of slow-spreading oceanic lithosphere. *Nature* **2008**, *455*, 790–794. [[CrossRef](#)]
19. Searle, R.C.; Bralee, A.V. Asymmetric generation of oceanic crust at the ultra-slow spreading Southwest Indian Ridge, 64° E. *Geochem. Geophys. Geosyst.* **2007**, *8*, Q05015. [[CrossRef](#)]
20. Zhang, T.; Gao, J.; Wang, W.; Wu, Z.; Shen, Z.; Yang, C. Asymmetric spreading rates and crustal structures of the Mohns Ridge since 20 Ma. *Chin. J. Geophys.* **2018**, *61*, 3263–3277. [[CrossRef](#)]
21. Stein, S.; Melosh, H.J.; Minster, J.B. Ridge migration and asymmetric sea-floor spreading. *Earth Planet. Sci. Lett.* **1977**, *36*, 51–62. [[CrossRef](#)]
22. Müller, R.D.; Roest, W.R.; Royer, J.-Y. Asymmetric sea-floor spreading caused by ridge–plume interactions. *Nature* **1998**, *396*, 455–459. [[CrossRef](#)]
23. Müller, R.D.; Sdrolias, M.; Gaina, C.; Roest, W.R. Age, spreading rates, and spreading asymmetry of the world’s ocean crust. *Geochem. Geophys. Geosyst.* **2008**, *9*, Q04006. [[CrossRef](#)]

24. Cannat, M.; Rommevaux-Jestin, C.; Fujimoto, H. Melt supply variations to a magma-poor ultra-slow spreading ridge (Southwest Indian Ridge 61° to 69° E). *Geochem. Geophys. Geosyst.* **2003**, *4*, 9104. [[CrossRef](#)]
25. Liang, Y.; Li, J.; Li, S.; Ni, J.; Ruan, A. The Magmato-tectonic dynamic model for the Indomed-Gallieni segment of the central southwest Indian ridge. *Chin. J. Geophys.* **2014**, *57*, 2993–3005. [[CrossRef](#)]
26. Wang, D.; Li, J.; Li, Y. Rheology of the lower crust controls the polarity of conjugated basins asymmetry on the South Atlantic passive margin. *Earth Sci. Front.* **2020**, *27*, 254. [[CrossRef](#)]
27. Johansen, S.E.; Panzner, M.; Mittet, R.; Amundsen, H.E.F.; Lim, A.; Vik, E.; Landrø, M.; Arntsen, B. Deep electrical imaging of the ultraslow-spreading Mohns Ridge. *Nature* **2019**, *567*, 379–383. [[CrossRef](#)] [[PubMed](#)]
28. Murton, B.J.; Baker, E.T.; Sands, C.M.; German, C.R. Detection of an unusually large hydrothermal event plume above the slow-spreading Carlsberg Ridge: NW Indian Ocean. *Geophys. Res. Lett.* **2006**, *33*, L10608. [[CrossRef](#)]
29. Schmidt-Aursch, M.C.; Jokat, W. 3D gravity modelling reveals off-axis crustal thickness variations along the western Gakkell Ridge (Arctic Ocean). *Tectonophysics* **2016**, *691*, 85–97. [[CrossRef](#)]
30. Wang, T.; Tucholke, B.E.; Lin, J. Spatial and temporal variations in crustal production at the Mid-Atlantic Ridge, 25° N–27°30' N and 0–27 Ma. *J. Geophys. Res. Solid Earth* **2015**, *120*, 2119–2142. [[CrossRef](#)]
31. Yang, C.; Han, X.; Wang, Y.; Li, H.; Qiu, Z.; Wu, Z. Characteristics of the multibeam backscatter of Carlsberg Ridge (60°–61° E) and its indication on the tectonics and magmatism. *J. Mar. Sci.* **2018**, *36*, 37–49. [[CrossRef](#)]
32. Mittelstaedt, E.; Ito, G.; van Hunen, J. Repeat ridge jumps associated with plume-ridge interaction, melt transport, and ridge migration. *J. Geophys. Res. Solid Earth* **2011**, *116*, B01102. [[CrossRef](#)]
33. Brozena, J.M.; White, R.S. Ridge jumps and propagations in the South Atlantic Ocean. *Nature* **1990**, *348*, 149–152. [[CrossRef](#)]
34. Bruguier, N.; Minshull, T.; Brozena, J. Morphology and tectonics of the Mid-Atlantic Ridge, 7°–12° S. *J. Geophys. Res. Solid Earth* **2003**, *108*, 2093. [[CrossRef](#)]
35. Mittelstaedt, E.; Ito, G.; Behn, M.D. Mid-ocean ridge jumps associated with hotspot magmatism. *Earth Planet. Sci. Lett.* **2008**, *266*, 256–270. [[CrossRef](#)]
36. Mittelstaedt, E.; Soule, S.; Harpp, K.; Fornari, D.; McKee, C.; Tivey, M.; Geist, D.; Kurz, M.D.; Sinton, C.; Mello, C. Multiple expressions of plume-ridge interaction in the Galápagos: Volcanic lineaments and ridge jumps. *Geochem. Geophys. Geosyst.* **2012**, *13*, Q05018. [[CrossRef](#)]
37. Li, X.; Kind, R.; Yuan, X.; Wölbern, I.; Hanka, W. Rejuvenation of the lithosphere by the Hawaiian plume. *Nature* **2004**, *427*, 827–829. [[CrossRef](#)] [[PubMed](#)]
38. Li, J.; Zhang, H.; Li, H.; Liu, Z. Mid-ocean Ridge Jump and Extension in the Context of Hotspots: Discussion on the Tectonic Evolution of Indian Ocean. *Geol. J. China Univ.* **2016**, *22*, 74.
39. Artemieva, I.M.; Yang, H.; Thybo, H. Incipient ocean spreading beneath the Arabian shield. *Earth-Sci. Rev.* **2022**, *226*, 103955. [[CrossRef](#)]
40. Huang, C.; Wang, P.; Yu, M.; You, C.; Liu, C.S.; Zhao, X.; Shao, L.; Zhong, G.; Yumul, G.P.J. Potential role of strike-slip faults in opening up the South China Sea. *Natl. Sci. Rev.* **2019**, *6*, 891–901. [[CrossRef](#)]
41. Hall, R. Cenozoic geological and plate tectonic evolution of SE Asia and the SW Pacific: Computer-based reconstructions, model and animations. *J. Asian Earth Sci.* **2002**, *20*, 353–431. [[CrossRef](#)]
42. Sibuet, J.-C.; Yeh, Y.-C.; Lee, C.-S. Geodynamics of the South China Sea. *Tectonophysics* **2016**, *692*, 98–119. [[CrossRef](#)]
43. Briais, A.; Patriat, P.; Tapponnier, P. Updated interpretation of magnetic anomalies and seafloor spreading stages in the South China Sea: Implications for the Tertiary tectonics of Southeast Asia. *J. Geophys. Res. Solid Earth* **1993**, *98*, 6299–6328. [[CrossRef](#)]
44. Taylor, B.; Hayes, D.E. Origin and History of the South China Sea Basin. In *The Tectonic and Geologic Evolution of Southeast Asian Seas and Islands: Part 2*; American Geophysical Union: Washington, DC, USA, 1983; Volume 27, pp. 23–56.
45. Li, J. Dynamics of the continental margins in South China Sea: Scientific experiments and research progresses. *Chin. J. Geophys.* **2011**, *54*, 883–893. [[CrossRef](#)]
46. Qin, X.; Zhang, B.; Zhao, B. Distribution characteristics of Mohorovicic discontinuity in the South China Sea Basin and suggestions for drilling preparation area. *Acta Geol. Sin.* **2022**, *96*, 2635–2646. [[CrossRef](#)]
47. Qin, X.; Zhao, B.; Li, F.; Zhang, B.; Wang, H.; Zhang, R.; He, J.; Chen, X. Deep structural research of the South China Sea: Progresses and directions. *China Geol.* **2019**, *2*, 530–540. [[CrossRef](#)]
48. Ren, J.; Luo, P.; Gao, Y.; Wang, H.; Lei, C.; Chao, P. Structural, sedimentary and magmatic records during continental breakup at southwest sub-basin of South China Sea. *Earth Sci.* **2022**, *47*, 2287–2302. [[CrossRef](#)]
49. Lei, C.; Alves, T.M.; Ren, J.; Pang, X.; Yang, L.; Liu, J. Depositional architecture and structural evolution of a region immediately inboard of the locus of continental breakup (Liwán Sub-basin, South China Sea). *GSA Bull.* **2019**, *131*, 1059–1074. [[CrossRef](#)]
50. Fan, Q.; Li, J.; Liu, C.; Pan, X. In-Fluence over Migration of MOR Spreading Center from Detachment Faults of Mid-Ocean Ridges and Development of Oceanic Core Complex. *Acta Geol. Sin.* **2018**, *92*, 2040–2050.
51. Li, H.; Zheng, J.; Pang, X.; Ren, J.; Li, R. Structural Patterns and Controlling Factors of Differential Detachment in the Northern Continental Margin of the South China Sea: Taking Baiyun-Liwán Deep Water Area in the Pearl River Mouth Basin as an Example. *China Offshore Oil Gas* **2020**, *32*, 24–35. [[CrossRef](#)]

52. Ren, J.; Pang, X.; Yu, P.; Lei, C.; Luo, P. Characteristics and formation mechanism of deepwater and ultra-deepwater basins in the northern continental margin of the South China Sea. *Chin. J. Geophys.* **2018**, *61*, 4901–4920. [[CrossRef](#)]
53. Ren, J.; Pang, X.; Lei, C.; Yuan, L.; Liu, J.; Yang, L. Ocean and continent transition in passive continental margins and analysis of lithospheric extension and breakup process: Implication for research of the deepwater basins in the continental margins of South China Sea. *Earth Sci. Front.* **2015**, *22*, 102. [[CrossRef](#)]
54. Wang, P. Tracing the life history of a marginal sea—On “The South China Sea Deep” research program. *Chin. Sci. Bull.* **2012**, *57*, 3093–3114. [[CrossRef](#)]
55. Yao, B.; Zeng, W.; Hayes, D.E. *The Geological Memoir of South China Sea Surveyed Jointly by China and USA*; China University of Geosciences Press: Wuhan, China, 1994.
56. Li, C.-F.; Xu, X.; Lin, J.; Sun, Z.; Zhu, J.; Yao, Y.; Zhao, X.; Liu, Q.; Kulhanek, D.K.; Wang, J.; et al. Ages and magnetic structures of the South China Sea constrained by deep tow magnetic surveys and IODP Expedition 349. *Geochem. Geophys. Geosyst.* **2014**, *15*, 4958–4983. [[CrossRef](#)]
57. Ben-Avraham, Z.; Uyeda, S. The evolution of the China Basin and the mesozoic paleogeography of Borneo. *Earth Planet. Sci. Lett.* **1973**, *18*, 365–376. [[CrossRef](#)]
58. Taylor, B.; Hayes, D.E. The Tectonic Evolution of the South China Basin. In *The Tectonic and Geologic Evolution of Southeast Asian Seas and Islands: Part 1*; American Geophysical Union: Washington, DC, USA, 1980; Volume 23, pp. 89–104.
59. Li, C.F.; Li, J.; Ding, W.; Franke, D.; Yao, Y.; Shi, H.; Pang, X.; Cao, Y.; Lin, J.; Kulhanek, D.K. Seismic stratigraphy of the central South China Sea basin and implications for neotectonics. *J. Geophys. Res. Solid Earth* **2015**, *120*, 1377–1399. [[CrossRef](#)]
60. Barckhausen, U.; Roeser, H.A. Seafloor spreading anomalies in the South China Sea revisited. *Cont. -Ocean Interact. Within East Asian Marg. Seas* **2004**, *149*, 121–125. [[CrossRef](#)]
61. Barckhausen, U.; Engels, M.; Franke, D.; Ladage, S.; Pubellier, M. Evolution of the South China Sea: Revised ages for breakup and seafloor spreading. *Mar. Pet. Geol.* **2014**, *58*, 599–611. [[CrossRef](#)]
62. Lin, J.; Li, J.; Xu, Y.; Sun, Z.; Xia, S.; Huang, X.; Xie, X.; Li, C.; Ding, W.; Zhou, Z.; et al. Ocean drilling and major advances in marine geological and geophysical research of the South China Sea. *Acta Oceanol. Sin.* **2019**, *41*, 125–140. [[CrossRef](#)]
63. Li, J.; Ding, W.; Gao, J.; Wu, Z.; Zhang, J. Cenozoic evolution model of the sea-floor spreading in South China Sea: New constraints from high resolution geophysical data. *Chin. J. Geophys.* **2011**, *54*, 894–906. [[CrossRef](#)]
64. Li, J.; Ding, W.; Wu, Z.; Zhang, J.; Dong, C. The propagation of seafloor spreading in the southwestern subbasin, South China Sea. *Chin. Sci. Bull.* **2012**, *57*, 3182–3191. [[CrossRef](#)]
65. Li, C.; Li, Z.; Li, Y.; Liu, Y.; Peng, X.; Wen, Y. Large Geological Differences between the East and Southwest Subbasins of the South China Sea. *Sci. Technol. Rev.* **2020**, *38*, 40–45. [[CrossRef](#)]
66. Ren, J.; Lei, C. Tectonic stratigraphic framework of Yinggehai-Qiongdongnan Basins and its implication for tectonic province division in South China Sea. *Chin. J. Geophys.* **2011**, *54*, 3303–3314. [[CrossRef](#)]
67. Wang, W.; Yao, Y.; Cai, Z.; Yin, Z.; Zhu, R.; Wei, J.; Ju, D. Characteristics of unconformity T5 and T3 in the Zhongjiannan basin and their significance for scientific drilling in the South China Sea during the post-spreading period. *Acta Geol. Sin.* **2022**, *96*, 11. [[CrossRef](#)]
68. Li, C.; Song, T. Magnetic recording of the Cenozoic oceanic crustal accretion and evolution of the South China Sea basin. *Chin. Sci. Bull.* **2012**, *57*, 3165–3181. [[CrossRef](#)]
69. Ding, W.; Sun, Z.; Dadd, K.; Fang, Y.; Li, J. Structures within the oceanic crust of the central South China Sea basin and their implications for oceanic accretionary processes. *Earth Planet. Sci. Lett.* **2018**, *488*, 115–125. [[CrossRef](#)]
70. Ding, H.; Ding, W.; Zhang, F.; Wu, Z.; Yin, S.; Fang, Y. Asymmetric Deep Structure of the South China Sea Basin and Its Controlling Factors. *Earth Sci.* **2021**, *46*, 929–941. [[CrossRef](#)]
71. Zhang, F.; Lin, J.; Zhang, X.; Ding, W.; Wang, T.; Zhu, J. Asymmetry in oceanic crustal structure of the South China Sea basin and its implications on mantle geodynamics. *Int. Geol. Rev.* **2020**, *62*, 840–858. [[CrossRef](#)]
72. Lin, J.; Xu, Y.; Sun, Z.; Zhou, Z. Mantle upwelling beneath the South China Sea and links to surrounding subduction systems. *Natl. Sci. Rev.* **2019**, *6*, 877–881. [[CrossRef](#)] [[PubMed](#)]
73. Wen, Y.; Li, C.-F.; Wang, L.; Liu, Y.; Peng, X.; Yao, Z.; Yao, Y. The onset of seafloor spreading at the northeastern continent-ocean boundary of the South China Sea. *Mar. Pet. Geol.* **2021**, *133*, 105255. [[CrossRef](#)]
74. Guan, Q.; Zhang, T.; Taylor, B.; Gao, J.; Li, J. Ridge jump reorientation of the South China Sea revealed by high-resolution magnetic data. *Terra Nova* **2021**, *33*, 475–482. [[CrossRef](#)]
75. Ding, W. Continental margin dynamics of South China Sea: From continental break-up to seafloor spreading. *Earth Sci.* **2021**, *46*, 790–800. [[CrossRef](#)]
76. Xu, H.; Ma, H.; Song, H.; Chen, A. Numerical simulation of Eastern South China Sea basin expansion. *Chin. J. Geophys.* **2011**, *54*, 3070–3078. [[CrossRef](#)]
77. Key, K.; Constable, S.; Liu, L.; Pommier, A. Electrical image of passive mantle upwelling beneath the northern East Pacific Rise. *Nature* **2013**, *495*, 499–502. [[CrossRef](#)] [[PubMed](#)]
78. Li, F.; Gao, Y. The first ultra deep water electromagnetic survey across the paleo spreading ridge of the South China Sea has been successfully completed. *Chin. Sci. Bull.* **2021**, *66*, 2. [[CrossRef](#)]
79. Zelt, C.A.; Smith, R.B. Seismic travelttime inversion for 2-D crustal velocity structure. *Geophys. J. Int.* **1992**, *108*, 16–34. [[CrossRef](#)]

80. Qiu, X.; Zhao, M.; Xu, H.; Li, J.; Ruan, A.; Hao, T.; You, Q. Important processes of deep seismic surveys in the South China Sea: Retrospection and expectation. *J. Trop. Oceanogr.* **2012**, *31*, 1–9.
81. Zhao, M.; Qiu, X.; Xu, H.; Xia, S.; Wu, Z.; Li, J. Deep seismic surveys in the southern South China Sea and contrast on its conjugate margins. *Earth Sci.* **2011**, *36*, 823–830.

Disclaimer/Publisher’s Note: The statements, opinions and data contained in all publications are solely those of the individual author(s) and contributor(s) and not of MDPI and/or the editor(s). MDPI and/or the editor(s) disclaim responsibility for any injury to people or property resulting from any ideas, methods, instructions or products referred to in the content.